



Corrosion inhibitory action of ethanol extract from *Bagassa guianensis* on the corrosion of zinc in ASTM medium

M. Lebrini*, F. Suedile, C. Roos

Laboratoire Matériaux et Molécules en Milieux Amazonien, CNRS 8172-UMR ECOFOG Universités Antilles, Département Scientifique Interfacultaire, B.P. 7209 F - 97275 Schoelcher, Martinique, France

Received 22May 2017,
Revised 11Sep 2017,
Accepted 15Sep 2017

Keywords

- ✓ *Bagassa guianensis* extract;
- ✓ Neutral inhibition;
- ✓ Zinc;
- ✓ EIS and polarization;

Mounim Lebrini
mounim.lebrini@univ-antilles.fr

Abstract

Ethanol extract of *Bagassa guianensis* was tested as corrosion inhibitor for zinc in ASTM medium using polarization and electrochemical impedance spectroscopy (EIS). The results obtained show that this plant extract could serve as an effective inhibitor for the corrosion of zinc in sodium chloride media. The extract obtained give inhibition around 85%. Polarization curves show that *Bagassa guianensis* extract affects the anodic and cathodic reactions and the corrosion potential values were shifted to the positive potentials in the presence of the crude extract in the ASTM medium. The experimental data obtained from EIS method show a frequency distribution and therefore a modelling element with frequency dispersion behavior, a constant phase element (CPE _{α ,Q}) has been used. Graphical methods are illustrated by synthetic data to determine the parameter of CPE (α , Q). Studies on the phytochemical constituents of the total extract were also established. Electrochemical studies, on the chemical families present in the crude extract, were also carried out to find the main constituents responsible for corrosion inhibition properties of the plant extract.

1. Introduction

Use of inhibitors is one of the most practical methods for protection against corrosion especially in acid solutions to prevent metal dissolution and acid utilization [1]. Several studies have been published on the use of natural products as corrosion inhibitors in different media [2–6]. The significance of this area of research is primarily due to the fact that natural products are environmentally friendly and ecologically acceptable. Our research group has recently reported on the corrosion inhibitive effectiveness of C38 steel and zinc by some tropical plants [4–6]. *Bagassa guianensis* is a common wood from the north of South America. It is used in carpentry. *Bagassa guianensis* is found to contain sterols and flavonoids [7, 8]. However, it has never been studied for the purpose of corrosion inhibition. This study aims to gain some insight about the mode of action of ethanol extract from *Bagassa guianensis* plant (EEBGP) as a corrosion inhibitor of Zinc. The inhibitor effect of this naturally occurring biological molecules on the corrosion of zinc in an ASTM medium was investigated by potentiodynamic polarization and electrochemical impedance. Graphical techniques are used to determine the constant phase element parameters. Additionally, phytochemical and electrochemical studies of constituents of the total extract were established

2. Experimental details

2.1. Plant material and extraction

Leaves of *Bagassa guianensis* plant were collected on the area of Cayenne, dried during three weeks at temperate room and ground. The leaves of plant *Bagassa guianensis* were washed using water, shade dried, powdered into small pieces and the powdered leaves were extracted successively with ethanol (70%) from crude extracts using either heating under reflux or ultrasound assisted extraction (UAE). The extracted solution was then filtered and concentrated until the total ethanol from the extract evaporates. This solid extract was used to

prepare the required concentrations of *Bagassa guianensis* in order to study its effect as corrosion inhibitor for Zinc.

2.2 Separation and determination of organic compounds class

The phytochemical tests permits to identify the class of organic compounds present in the extract. For that purpose, specific reactions with the properties of each family were realized, according to a previously described experimental procedure [9,10]. Mayer, Wagner and Dragendroff tests were used to identify the presence of alkaloids. The presence of flavonoids and leucoanthocyanidin were referred to Bate-Smith and Wilstater tests. The ferric chloride test was used to determine the presence of tannin and some polyphenol. The presence of quinine was established by sodium hydroxide test. Lieberman-Burchard and Salkowski tests were used for Steroid and Triterpenes class. The separation was performed with a UHPLC-DAD Ultimate 3000 from Thermo Scientific. Preparative HPLC with fractions collection was used. A ramp gradient of water and acetonitrile as solvent and a C18 column was applied.

2.3 Electrochemical measurements

Corrosion tests have been carried out on electrodes cut from sheets of zinc. The specimens were embedded in epoxy resin leaving a working area of 1cm². The tested corrosive media is an ASTM media (148 mg/L Na₂SO₄, 138 mg/L NaHCO₃ and 165 g/L NaCl at a pH = 8.2). All the tests were performed at ambient temperature (25 °C). The concentration range of extract from *Bagassa guianensis* plant employed was 25 –100 mg L.

The electrochemical study was realized using a potentiostat VMP3 from Bio-Logic. The electrochemical measurements were performed in a three-electrode cell. The zinc was used as the working electrode, a platinum wire as the counter electrode and a saturated calomel electrode (SCE) as the reference electrode. Before each Tafel and EIS experiments, the electrode was allowed to corrode freely and its open-circuit potential (OCP) was recorded as a function of time during 3 h in ASTM solution, the time necessary to reach a quasi-stationary value of the open-circuit potential. This steady-state OCP corresponds to the corrosion potential (E_{corr}) of the working electrode.

The anodic and cathodic polarization curves were recorded by a constant sweep rate of 20 mV min⁻¹. Electrochemical impedance spectroscopy (EIS) measurements were carried out, using ac signals of amplitude 5 mV peak to peak at different conditions in the frequency range of 100 kHz to 10 mHz. The above procedures were triplicated for each concentration of tested inhibitor. The Tafel and EIS data were analysed using graphing and analyzing impedance software, version EC-Lab V10.20.

3. Results and Discussion

3.1. Extraction and characterization of plant extract

Two methods of extraction were used to obtain the extract plant; the first is ultrasound-assisted extraction and the second consists of heating under reflux. In these two methods a mixture of water ethanol (30/70) was used, which is the cheapest and greenest solvent. The reflux extraction method gives the highest yield (10.5 %). However no difference was observed in the composition of organic compounds present in the extract. Figure 1 shows the FTIR spectra of the extract obtained by both methods.

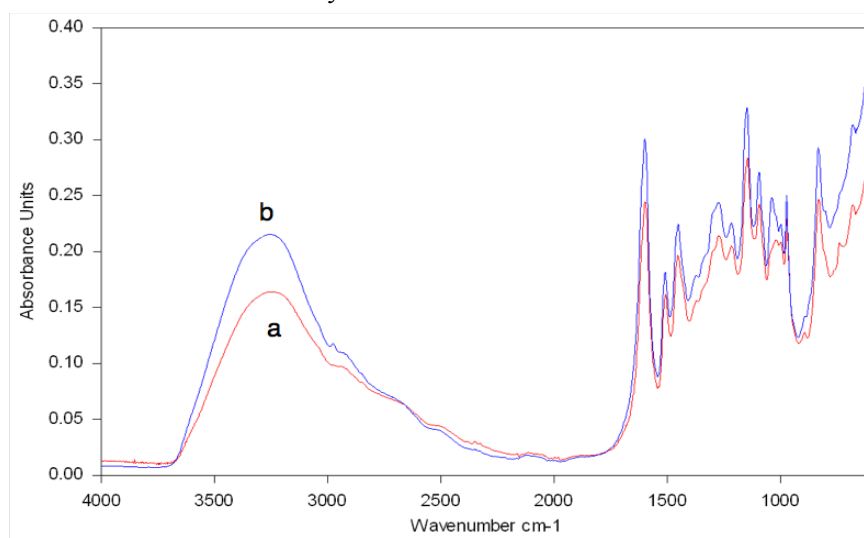


Figure 1: FT-IR spectra of EEBGP obtained by; (a) under reflux and (b) ultrasound-assisted extraction.

The analysis of the spectra shows almost similar characteristic bands of the *Bagassa guianensis* extract, confirming that the composition of organic compounds is the same in the two extracts whatever the extraction process used. HPLC chromatogram of total extract from *Bagassa guianensis* plant is shown in Figure 2. Similar results were found for the both extraction methods. It contains over 3 major peaks along with many small peaks indicating presence of more than 15 compounds. At this section of study, the total extract from *Badges guianensis* plant was used as such for corrosion inhibition studies.

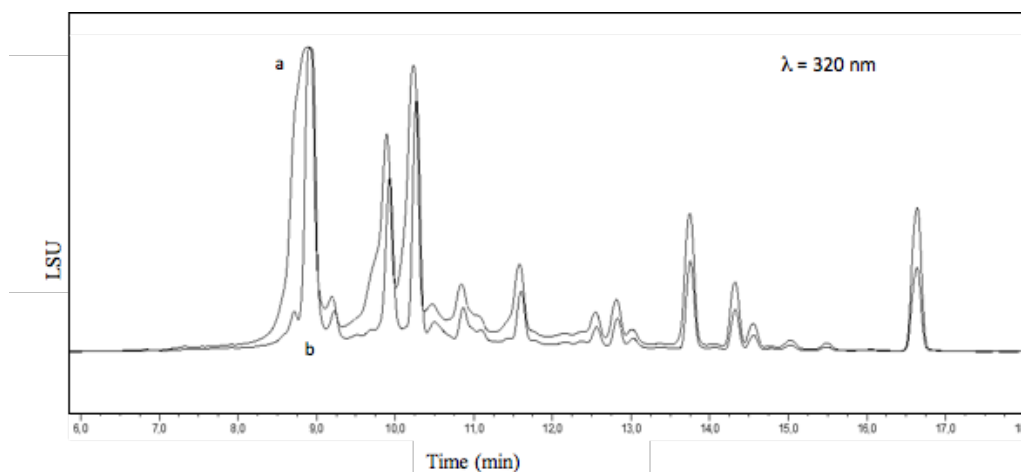


Figure 2: HPLC chromatogram of *EEBGP*; (a) reflux method and (b) ultrasound-assisted extraction method.

3.2. Linear Polarization:

Linear polarization method was used to evaluate the corrosion rate of zinc in the presence of *EEBGP*. Linear polarization curves of the zinc in the ASTM solution with or without addition of various concentrations of *EEBGP* are shown in Figure 3a for the extract obtained under reflux and in Figure 3b for the extract obtained using UAE. These figures show that the corrosion potential values were shifted to the negative values in the presence of the crude extract (from 10mV to 100mV), but has not been changed significantly with respect to inhibitor concentration. Therefore, we can say that the presence of *EEBGP* depressed the cathodic current. The inhibition efficiency (*IE*) is calculated using the equation 1 with the polarization resistance (*R_p*) values. The *R_p* values were obtained using linear *I*–*E* plots in the potential range ± 25 mV from the corrosion potential.

$$IE (\%) = \left[\frac{R_p - R_p^0}{R_p} \right] \times 100 \quad 1$$

Where R_p^0 and R_p are the polarization resistance values in the absence and presence of extract, respectively. The calculation with the Tafel curves is not possible as the experimental polarization curves do not exhibit linear Tafel regions. It can be seen from Table 1 that the polarization resistance increase and the *IE* (%) values increase with the *EEBGP* concentration. Moreover, the reflux extract seems to be more efficient than the UAE one indeed the inhibition values are higher when the reflux extraction method is used.

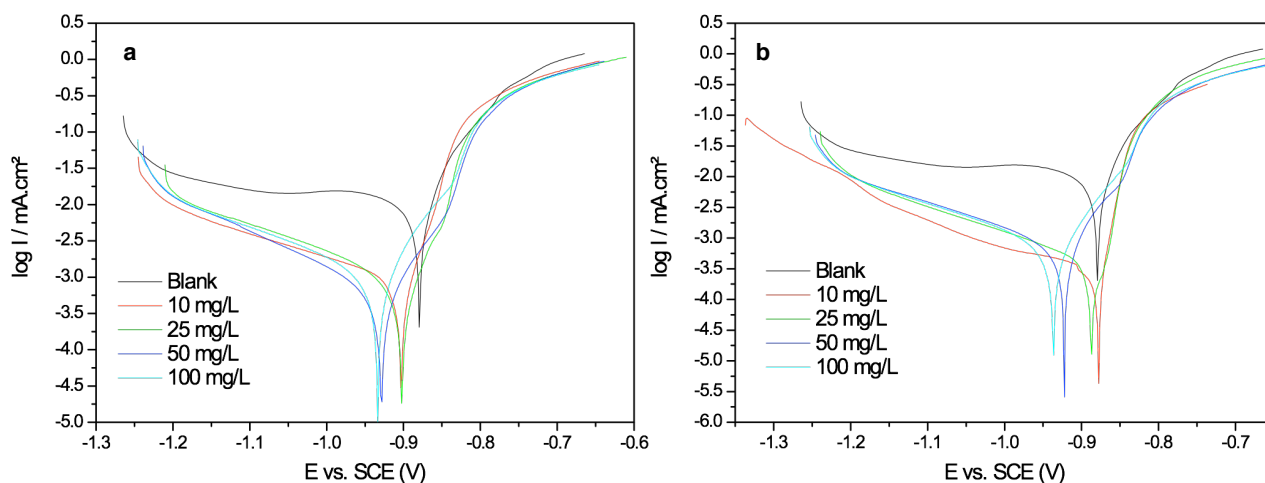


Figure 3: Polarization curves for zinc in the ASTM medium containing different concentrations of *EEBGP* obtained a) under reflux and b) by UAE.

Table 1: Polarization parameters and the corresponding inhibition efficiency for the corrosion of zinc in the ASTM medium containing different concentrations of *EEBGP* at 25 °C.

	<i>Concentration</i>	<i>E_{corr} vs. SCE (V)</i>	<i>R_p (Ω cm²)</i>	<i>IE (%)</i>
ASTM		-0.898	6 134	—
<i>UAE</i>	10 mg/L	-0.865	9 771	37
	25 mg/L	-0.905	20 241	70
	50 mg/L	-0.943	26 562	77
	100 mg/L	-0.896	30 477	80
<i>Reflux</i>	10 mg/L	-0.919	15 337	60
	25 mg/L	-0.886	20 273	70
	50 mg/L	-0.924	32 246	81
	100 mg/L	-0.918	38 497	84

3.3. Electrochemical Impedance Spectroscopy:

Different concentrations of the crude extracts of *Bagassa guianensis* were tested using electrochemical impedance spectroscopy in order to give evidence of the inhibitive activity of the plant extract. All the impedance spectra were measured at the corresponding open-circuit potentials. The Nyquist plots obtained, for zinc in the ASTM medium at 25°C containing different concentrations of *EEBGP*, are shown in Figure 4. The corresponding Bode plots are shown in Figures 5 and 6. All the Nyquist plots of zinc in the uninhibited and inhibited solutions present one capacitive loop and the corresponding Bode diagrams show one-time constant indicating a charge transfer phenomenon. However, at the concentration of 10 mg/L of *EEBGP*, the Nyquist diagram shows one depressed capacitive semicircle. The appearance of this depressed capacitive loop can be attributed to the dispersion of the points during the recording of the spectrum due to a sharp change in potential and are therefore not significant. Indeed, at low frequencies, the acquisition points last several minutes. Therefore, we used the equivalent circuit shown in Figure 7 to fit all our experimental impedance data. Increasing the extract concentration resulted in an increase in the impedance with frequency for both methods of extraction, Figure 6. The CPE is substituted for the capacitive element to give a more accurate fit as specified in the CPE impedance, equation 2.

$$Z_{CPE} = Q^{-1}(i\omega)^{-\alpha} \quad 2$$

Where Q is the CPE constant, ω is the angular frequency (in $\text{rad}\cdot\text{s}^{-1}$), $i^2 = -1$ is the imaginary number and α is a CPE exponent.

All the impedance parameters obtained from the experimental impedance data fit, including R_1 , R_2 , Q and α are shown in the Table 2 for the *UAE* extract and in the Table 3 for the *reflux* extract. The calculated inhibition efficiency according to the equation 3 is also given in the tables.

$$IE (\%) = \left[\frac{R_t - R_t^0}{R_t} \right] \times 100 \quad 3$$

Where R_t^0 and R_t are respectively the charge transfer resistance in the absence and presence of extract.

The "double layer capacitance" values (C_{dl}) were calculated using the Hsu and Mansfeld formula, equation 4. The Hsu and Mansfeld formula have been used to extract effective capacitance values from CPE parameters for studies on passive films [11-13], protective coatings [14-18] and corrosion inhibitors [19].

$$C_{dl} = (Q \times R_t^{1-\alpha})^{1/\alpha} \quad 4$$

The C_{dl} values are calculate from fit and graphical parameters. For more accurate of the CPE parameters α and Q were used to calculate the C_{dl} values, we graphically calculated these parameters from the impedance data for the phenomenon according to the graphical methods presented by Orazem et al. and Musiani et al. [20, 21]. First, we plotted on a logarithmic scale the imaginary part of the impedance as a function of frequency for the blank and each concentration of inhibitor to obtain $-\alpha$, Figure 8a. The obtained α is the value of the slope as given by the equation 5 according to Hirschorn et al. [22]. After that, for each frequency, we calculated the

effective capacity Q_{eff} according to the equation 6. Moreover, with the calculated values, we plotted the coefficient Q_{eff} as a function of frequency on a logarithmic scale, Figure 8b. The asymptote provides the correct value for the CPE coefficient Q . The results obtained by graphical method show one time constant too.

$$\alpha = \left| \frac{d \log|Z_i|}{d \log|Z_f|} \right| \quad 5$$

$$Q_{eff} = \sin\left(\frac{\alpha\pi}{2}\right) \frac{-1}{Z_i(f)(2\pi)^\alpha} \quad 6$$

The CPE parameters α and Q calculated for both uninhibited and inhibited solutions by the graphical method are summarized in Table 4. The calculated C_{dl} values are also shown in the same table.

From Tables 2 and 3, it can be seen that the R_l values have little changes upon addition of plant extract. The charge transfer resistance (R_t) values increase with the inhibitor concentration and remain unchanged upon addition of 50 mg/L for plant extract obtained by UAE. This increase in R_t leads an increase in the corrosion inhibition efficiency. The $IE(\%)$ values calculated from impedance study are in agreement with those obtained from polarization measurements. The α values are higher than that obtained for the corrosive solution; indicating a decreased heterogeneity of the zinc surface as a result of adsorption of extract molecules. The α values are almost independent of the concentration of the extract and remain unchanged upon addition of plant extract. The double layer formed at the electrode-solution interface is considered as an electric capacitor, whose capacitance decreases due to the displacement of water molecules and other ions originally adsorbed on the electrode by the extract molecules, forming a protective layer which decrease the number of actives sites necessary for the corrosion reaction.

The results obtained by both fit and graphical data, for the plant extract obtained by UAE, show the same tendency with a difference in numerical values (similar results were obtained for the plant extract obtained under reflux). This variation is due to the frequency range used for the reason that the value of α was dependent on the frequency at which the slope was evaluated.

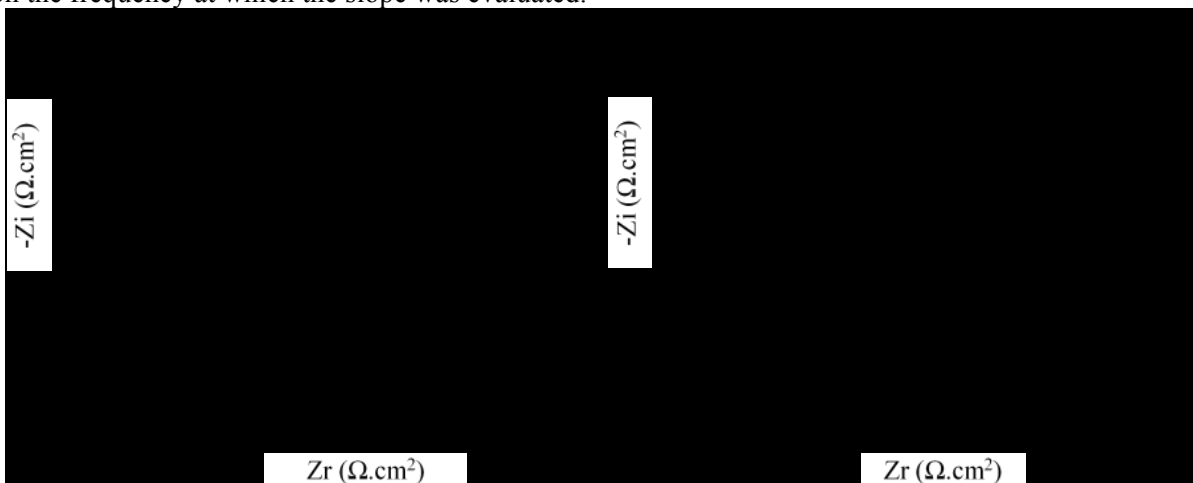


Figure 4: Nyquist plots for zinc in the ASTM medium containing different concentrations of *EEBGP* obtained a) under reflux and b) by UAE.

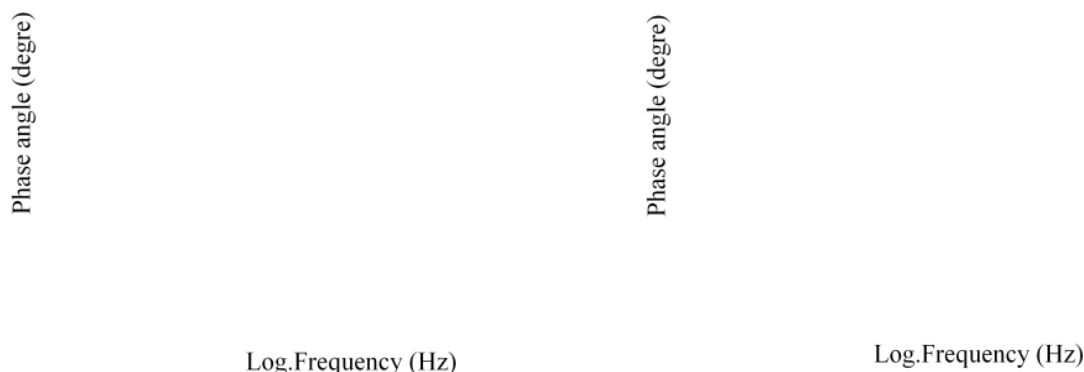


Figure 5: Bode plots, phase angle vs. freq for zinc in the ASTM medium containing different concentrations of *EEBGP* obtained a) under reflux and b) by UAE.

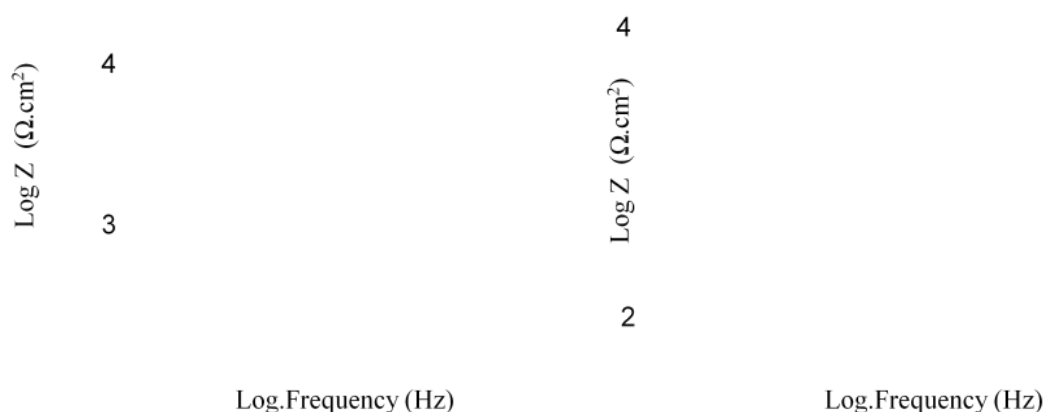


Figure 6: Bode plots, LogZ vs. freq for zinc in the ASTM medium containing different concentrations of *EEBGP* obtained a) under reflux and b) by UAE.

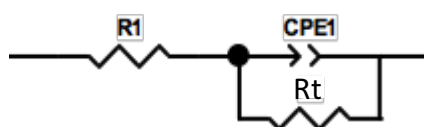


Figure 7:Equivalent circuit used to fit impedance data

Table 2: Values of the fit obtained from the EIS data for zinc in the ASTM medium with and without different concentrations of *EEBGP* obtained by UAE.

Parameters	Blank	10 mg/L	25 mg/L	50 mg/L	100 mg/L
$R_1(\Omega.cm^2)$	217	113	224	321	225
$Q_1 10^{-4}(\Omega^{-1}cm^{-2}s^\alpha)$	0.4	0.17	0.11	0.07	0.10
α_1	0.671	0.713	0.836	0.793	0.828
$R_t(\Omega.cm^2)$	1 876	10 202	21 066	25 175	24 547
$C_{dl}(\mu F cm^{-2})$	11	8	8	4	8
θ	-	0.8116	0.9109	0.9258	0.9236
IE (%)	-	82	91	92	92

Table 3: Values of the fit obtained from the EIS data for zinc in the ASTM medium with and without different concentrations of *EEBGP* obtained under reflux.

Parameters	Blank	10 mg/L	25 mg/L	50 mg/L	100 mg/L
$R_1(\Omega.cm^2)$	217	238	278	235	360
$Q_1 10^{-4}(\Omega^{-1}cm^{-2}s^\alpha)$	0.4	0.15	0.16	0.17	0.17
α_1	0.671	0.674	0.723	0.729	0.754
$R_t(\Omega.cm^2)$	1 876	9 107	18 789	29 659	34 772
$C_{dl}(\mu F cm^{-2})$	11	6	10	13	14
θ	-	0.7940	0.9001	0.9367	0.9460
IE (%)	-	79	90	94	95

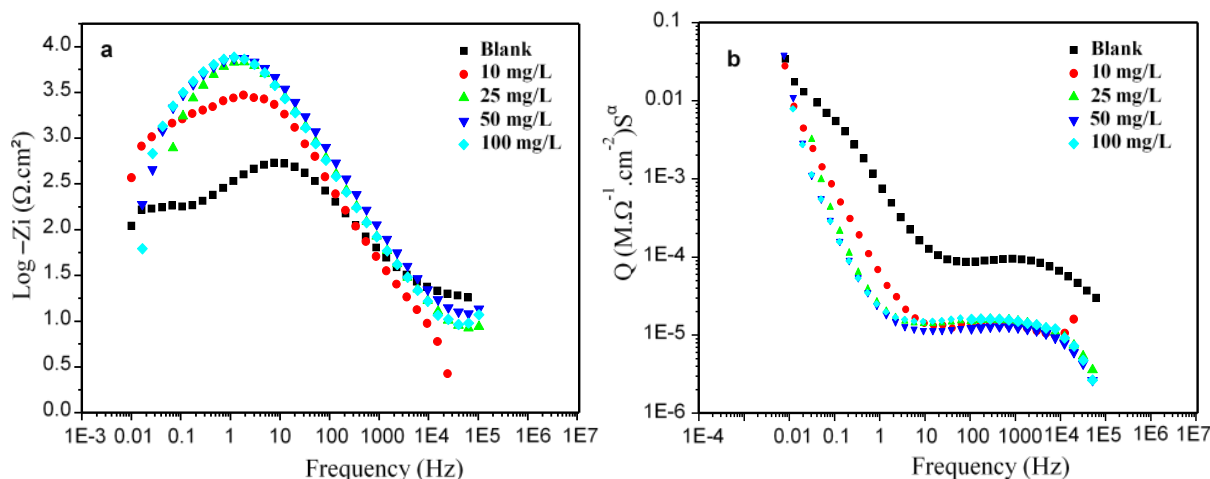


Figure 8: a) Imaginary part of the impedance as function of frequency b) Effective CPE coefficient for zinc in the ASTM medium with and without different concentrations of *EEBGP* obtained by UAE.

Table 4: Values of the graphical method obtained from the EIS data for zinc in the ASTM medium with and without different concentrations of *EEBGP* obtained by UAE.

Parameters	Blank	10 mg/L	25 mg/L	50 mg/L	100 mg/L
$Q_1 10^{-4} (\Omega^{-1} \text{cm}^{-2} \text{s}^{\alpha})$	0.9	0.1	0.1	0.1	0.2
α_1	0.5651	0.8413	0.7906	0.7782	0.7907
$C_{dl} (\mu\text{F cm}^{-2})$	4.07	2.78	1.98	1.95	5.24

3.4. Constituent responsible for inhibition

To improve our knowledge about the crude extract and its efficiency, three studies were combined to evaluate, quantify and qualify the use extract. The first one employ the phytochemical tests to qualify the different chemical families present in our extract, the second one to separate and quantify these different chemical families. In addition, the last one to compare the inhibition provided by crude extract constituents to find the main constituent responsible for corrosion inhibition properties of the plant extract.

3.4.1. Phytochemical tests and separation

Phytochemical tests are realized on the crude extract to determine the different chemical families. The tests used, according to Grenand [9], reveal the presence of many families: anthocyanins, coumarins, flavonoids, quinones, saponins, tannins and triterpens. To determine the proportion of each family, a separation was carried by a UHPLC and by a preparative column with a ramp gradient of water and acetonitrile as eluents. Seven fractions corresponding to the different chemical families present in the extract were isolated, collected and weighted. These fractions were submitted to phytochemical tests in order to confirm that each family was isolated separately. HPLC spectroscopy spectrum shows that each fraction contained a mixture of many compounds (Figure 9; representative example).

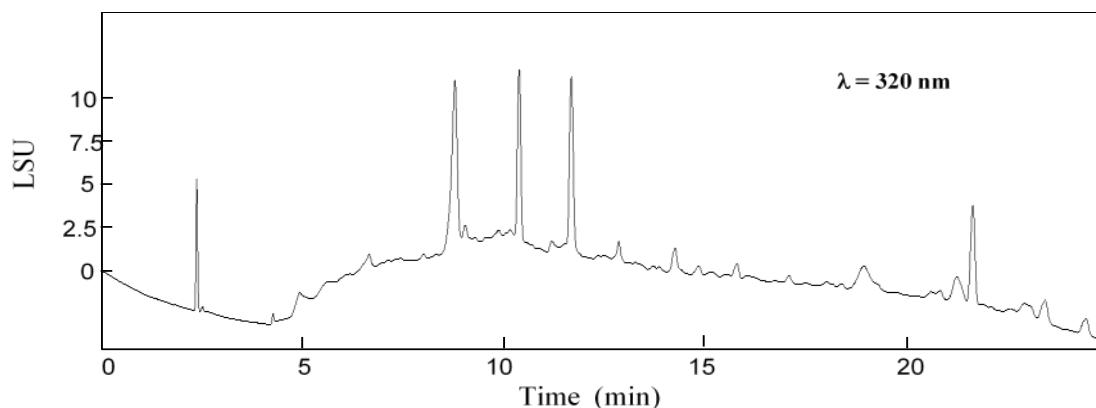


Figure 9: HPLC chromatogram of total anthocyanins extract from the crude extract.

Similar results were found for the others fractions. Since retention time of compounds is close to each other and it is very difficult to separate them, hence the every family was used as such for electrochemical studies. Table 5 regroupes the percentage of these different families in the total extract. To confirm these results, we realized directly a typical extraction for each family from the crude extract and every family extraction was collected and weighted, the percentage obtained from both techniques shows the same trend. The concentration range of each family employed as inhibitor was the average of the two techniques.

3.4.2. Electrochemical study

Figure 10 shows the Nyquist plots of zinc in the ASTM solution in absence and presence of crude extract and each family present in the extract at 25 °C. The electrochemical test was realized with a concentration of 20 mg/L of crude extract and this concentration was compared with each family present in the extract (the concentration of different families was calculated from their percentage in the extract). All the impedance spectra obtained for the corrosion of zinc in the ASTM medium with inhibitor consist of one capacitive loop. It can be seen that, the size of the capacitive loop with inhibitor are larger than the loop of the blank. The equivalent circuit given in Figure 7 was used to fit the obtained experimental spectra. The parameters calculated for both uninhibited and inhibited solutions are summarized in Table 5. The charge transfer resistance in the presence of different families are higher than the R_c obtained for the uninhibited solution. These results show clearly that each family inhibits the corrosion. The study of the different families presents in the crude extract show that the saponins family has the best behavior in the crude extract. Nevertheless, the inhibition behavior of the crude extract is due to a synergic effect between the different detected families. These results give evidence that the main constituents responsible of the corrosion inhibition properties of the plant extract are the saponin family; this behavior is due to their chemical structure presenting heteroatoms and also to the fact that their content percentage in the crude extract is the highest.

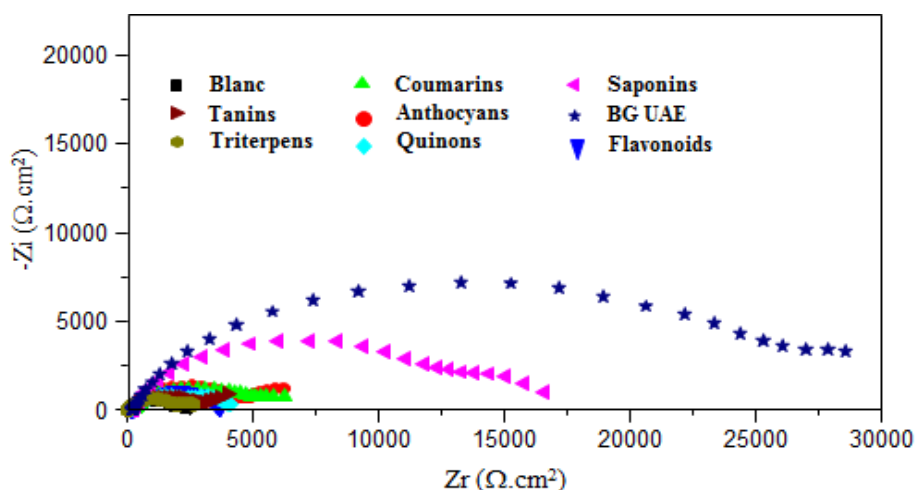


Figure 10: Nyquist plots for zinc in the ASTM medium containing different families and the crude extract.

Table 5: Values of the percentage of different families and the EIS data for zinc in the ASTM medium with and without inhibitor.

<i>Inhibitors</i>	<i>Thepercentage (%)</i>	<i>Concentration (mg/L)</i>	<i>R_c (Ω.cm²)</i>	<i>IE (%)</i>
<i>Blank</i>	-	-	1 876	-
<i>Anthocvans</i>	16	3.2	5 278	64
<i>Coumarins</i>	7	1.4	5 418	65
<i>Flavonoids</i>	23	4.5	3 650	49
<i>Quinons</i>	2	0.5	3 744	50
<i>Saponins</i>	36	7.3	14 788	87
<i>Tanins</i>	9	1.8	3 433	45
<i>Triterpens</i>	7	1.4	2 274	18
<i>Crude extract</i>	100	20	28 796	93

3.5. Adsorption behavior:

In order to study the isotherm adsorption behavior, the degree of surface coverage (θ) for the inhibitor was obtained from averaged EIS as follows:

$$\theta = \left[\frac{R_t - R_t^0}{R_t} \right] \quad 7$$

Where R_t^0 and R_t are the charge transfer resistance in the absence and presence of extract, respectively. Many adsorption isotherms were plotted and the Langmuir adsorption isotherm was found to be the best description of the adsorption behavior of the studied inhibitor. According to this isotherm, θ is related to the concentration of inhibitor in molarity via:

$$\text{Langmuir:} \quad \frac{C_{inh}}{\theta} = \frac{1}{K} + C_{inh} \quad 8$$

$$\text{Temkin:} \quad \exp(-2a\theta) = bC_{inh} \quad 9$$

$$\text{Frumkin:} \quad \left(\frac{\theta}{1-\theta} \right) \exp(-2a\theta) = bC_{inh} \quad 10$$

The plot of C_{inh}/θ versus C_{inh} gave a straight line as shown in Figure 11. The linear regression coefficient (R^2) is equal to 0.9999 for the UAE extract and to 0.9995 for the reflux extract, confirming that the adsorption of studied extract plant in ASTM solution follows the Langmuir's adsorption isotherm.

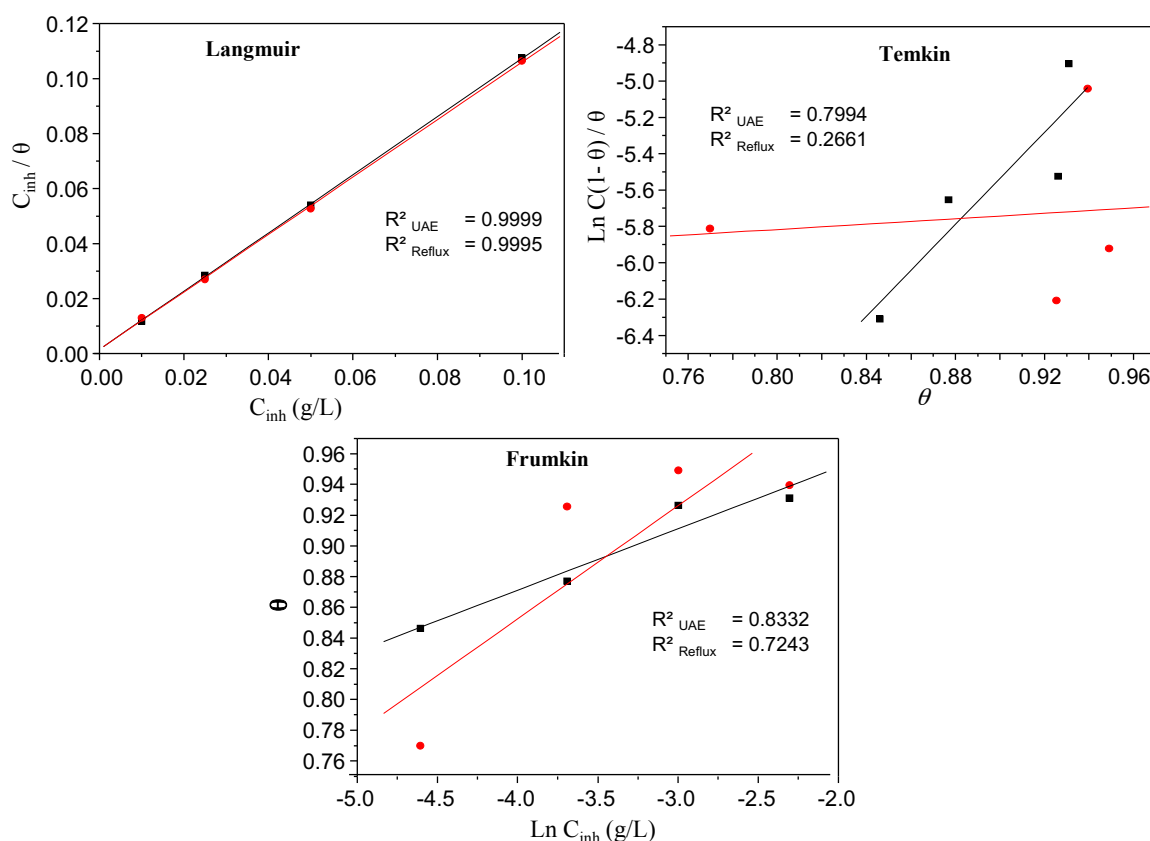


Figure 11: isotherm adsorption for zinc in the ASTM medium containing different concentration of *EEBGP* obtained under reflux and by UAE.

Conclusions

In this paper, we demonstrated that *Bagassa guianensis* extract is a good inhibitor of corrosion for zinc in sodium chloride solution. The polarization study showed *Bagassa guianensis* extract is a mixed-type inhibitor. The impedance study presented one-time constant corresponding to charge-transfer at the interface electrolyte/metal. The two methods used to calculate the CPE parameters showed the same trend. The adsorption behavior of studied extract plant follows the Langmuir's adsorption isotherm theory. Phytochemical tests reveal the presence of many families like anthocyanins, saponins, flavonoids, quinones, triterpens and

coumarins. The study of the different families presents in the crude extract show that the families have the same behavior as the crude extract. Nevertheless, the inhibition behavior of the crude extract is due to the presence of saponins family in the crude extract.

Acknowledgments-The authors are pleased to acknowledge MOM (Ministère des Outre-Mer) for providing the financing of their research.

References

1. J. Sykes, *Br. Corros. J.* 25 (1990) 175.
2. A.M. Abdel-Gaber, B.A. Abd-El-Nabey, M. Saadawy, *Corros. Sci.* 51 (2009) 1038.
3. F. ElHajjaji, H. Greche, M. Taleb, A. Chetouani, A. Aouniti, B. Hammouti, *J. Mater. Environ. Sci.* 7 (2) (2016) 566-578.
4. F. Suedile, F. Robert, C. Roos, M. Lebrini, *Electrochim. Acta* 133 (2014) 631.
5. M. Chevalier, C. Roos, F. Tomi, S. Sutour, M. Lebrini, *ECS Transactions* 64 (2015) 1.
6. M. Faustin, A. Maciuk, P. Salvin, C. Roos, M. Lebrini, *Corros. Sci.* 92 (2015) 287.
7. M. Royer, H. Herbette G., Beauchêne J., Thibaut B., *Phytochemistry* 71 (2010) 1708.
8. M. Royer, A.M.S. Rodrigues, G. Herbette, J. Beauchêne, M. Chevalier, B. Hérault, B. Thibaut, *Biodegradation* 70 (2012) 55.
9. P. Grenand, C. Moretti, H. Jacquemin, M. Prevost, *Pharmacopées traditionnelles en Guyane: Créoles, Wayapi, Palikur, IRD, Paris* (2004).
10. J.A. Botosoa, *Purification et Caractérisation chimique et biologique des principes actifs des extraits de feuilles de Pechiamadagascariensis (Apocynaceae)*, in: *Biochimie Fondamentale et Appliquée, Université d'Antananarivo*, (2010).
11. S.P. Harrington, T.M. Devine, *J. Electrochem. Soc.* 155 (2008) C381.
12. S.P. Harrington, T.M. Devine, *J. Electrochem. Soc.* 156 (2009) C154.
13. V.D. Jovic, B.M. Jovic, *Corros. Sci.* 50 (2008) 3063.
14. C.E. Barchiche, E. Rocca, J. Hazan, *Surf. Coat. Technol.* 202 (2008) 4145.
15. T. Van Schaftinghen, C. Le Pen, H. Terryn, F. Hörzenberger, *Electrochim. Acta* 49 (2004) 2997.
16. M.L. Zheludkevich, R. Serra, M.F. Montemor, K.A. Yasakau, I.M.M. Salvado, M.G.S. Ferreira, *Electrochim. Acta* 51 (2005) 208.
17. T. Van Schaftinghen, C. Deslouis, A. Hubin, H. Terryn, *Electrochim. Acta* 51 (2006) 1695.
18. K.A. Yasakau, M.L. Zheludkevich, O.V. Karavai, M.G.S. Ferreira, *Prog. Org. Coat.* 63 (2008) 352.
19. M.L. Zheludkevich, K.A. Yasakau, S.K. Poznyak, M.G.S. Ferreira, *Corros. Sci.* 47 (2005) 3368.
20. M.E. Orazem, N. Pébère, B. Tribollet, *J. Electrochem. Soc.* 153 (2006) B129.
21. M. Musiani, M.E. Orazem, B. Tribollet, V. Vivier, *Electrochim. Acta* 56 (2011) 8014.
22. B. Hirschorn, M.E. Orazem, B. Tribollet, V. Vivier, I. Frateur, M. Musiani, *Electrochim. Acta* 55 (2010) 6218.

(2018) ; <http://www.jmaterenvironsci.com>